

Cellular and nuclear morphological variability within a single species of the toxigenic dinoflagellate genus *Gambierdiscus*: Relationship to life-cycle processes



Isabel Bravo^{a,*}, Rosa Isabel Figueroa^{a,b}, Santiago Fraga^a

^a *Microalgas Nocivas (VGO-HAB), Instituto Español de Oceanografía (IEO), Subida a Radio Faro 50, 36390 Vigo, Spain*

^b *Aquatic Ecology, Biology Building, Lund University, 22362 Lund, Sweden*

ARTICLE INFO

Article history:

Received 14 August 2014

Received in revised form 30 September 2014

Accepted 30 September 2014

Available online

Keywords:

Gambierdiscus

Ciguatera fish poisoning

CFP

Benthic dinoflagellates

Harmful algae

Life cycle

ABSTRACT

Dinoflagellates belonging to the genus *Gambierdiscus* are the causative agent of ciguatera fish poisoning (CFP). This syndrome, which is widespread in tropical and subtropical regions, has recently been reported also in temperate latitudes. Taxonomic studies of *Gambierdiscus* have yet to completely couple the morphological features of member species with their genetics. In this study, the cellular and nuclear morphology of a single strain of one species of *Gambierdiscus* was determined in cells grown under different culture conditions. The results showed a wide-ranging variability of cell sizes, together with a clear relationship between cell size and nuclear morphology. Thus, small cells were associated with round to oval or slightly U-shaped nuclei and large cells with obviously U-shaped nuclei. Most cells exhibited the typical antero-posteriorly compressed lenticular, shape of *Gambierdiscus*, with the exception of a few small globular-shaped specimens. In all cells, regardless of their size, the arrangement of the thecal plates was typical of lenticular *Gambierdiscus*. Dividing cells were consistently the largest. In these cells, nuclear morphology, karyokinesis, and cytokinesis were characterized. Cells underwent division only during the dark period, thus demonstrating their spontaneous synchronized division. Cellular forms related to the sexual cycle were also present in the cultures and included gamete pairs and putative meiotic planozygotes. The effect of the culture medium was studied by means of principal component analyses, which showed a positive correlation between the medium used and nuclear size and shape but not cell size.

© 2014 The Authors. Published by Elsevier B.V. This is an open access article under the CC BY-NC-ND license (<http://creativecommons.org/licenses/by-nc-nd/3.0/>).

1. Introduction

Gambierdiscus is a genus of benthic dinoflagellates and the causative agent of ciguatera, a toxin-mediated disease first reported in tropical-subtropical regions (the Caribbean Sea, the Hawaiian Islands, Australia, Southeast Asia and the Indian Ocean) but more recently also in temperate regions (the Canary Islands, the Mediterranean Sea, the Gulf of Mexico, and in the Atlantic Ocean off the coast of North Carolina) (GEOHAB, 2012). The consumption by humans of fish that have ingested *Gambierdiscus* results in potentially severe gastrointestinal and neurological symptoms.

Initially, only one species of *Gambierdiscus* was recognized, *Gambierdiscus toxicus* (also referred to simply as *Gambierdiscus* sp.) due to the difficulty of distinguishing species differences using

light microscopy. Nonetheless, in the original description of *Gambierdiscus toxicus* (Adachi and Fukuyo, 1979) and in subsequent studies, the high variability in cell size and shape, growth rates, toxin production, and genetics suggested the presence of cryptic species, as later demonstrated by genetic sequencing (Litaker et al., 2009).

In the 1990s, six other species distinct from *Gambierdiscus toxicus* were described (Faust, 1995; Holmes, 1998; Chinain et al., 1999), with the last study being the first to use genetic sequencing in the taxonomic determination of *Gambierdiscus*. More recently, taxonomic studies, including phylogeny, have clarified the phylogenetic relationship between *Gambierdiscus* species (Litaker et al., 2010) and thus clarified the link between their geographic distribution and the occurrence of ciguateric fish poisoning. To date, 14 species have been described, with their genetic identification, including relative ribotype, linked to the corresponding morphological description (Adachi and Fukuyo, 1979; Faust, 1995; Holmes, 1998; Chinain et al., 1999; Litaker et al., 2009; Fraga et al., 2011; Aligizaki et al., 2010; Kuno et al., 2010; Nishimura et al., 2014). However, because of the

* Corresponding author. Tel.: +34 986 492111; fax: +34 986 498626.
E-mail address: isabel.bravo@vi.ieo.es (I. Bravo).

morphological plasticity of *Gambierdiscus* species their accurate identification is difficult and the concordance between phenotype and genotype in the genus is not yet well resolved (Parsons et al., 2012). For example, the two recently divided daughter cells differ in their respective morphologies (Fraga et al., 2011). Moreover, little is known about the relationship between the life-cycle processes of *Gambierdiscus*, including but not limited to cell division, and its morphological variability. In fact, the need for studies on the life cycle of *Gambierdiscus* was cited in the report of the Core Research Project of GEOHAB: HABs in Benthic Systems (GEOHAB, 2012).

According to von Stosch, the full recognition of a species includes knowledge of its complete life cycle, a view that has been widely accepted in dinoflagellate research (Elbrächter, 2003; Bravo and Figueroa, 2014). The morphological features of dinoflagellate cysts are known to differ from those of vegetative stages, and in the very limited, ambiguous observations of *G. toxicus* described in the literature both sexuality and cyst formation have been suggested albeit not confirmed (Hokama et al., 1996).

In the present study, we carried out a detailed examination of the variation in nuclear shapes and cell sizes in a single strain of *Gambierdiscus* sp., established from a sample obtained from the Celebes Sea (SW Pacific Ocean). Phylogenetic studies have confirmed this strain as a new species, distinct from other *Gambierdiscus* species. The different cell-cycle stages in cultures of this strain were monitored by nuclear staining. In addition, cell sizes were measured in different enriched media. In total, 1315 specimens were studied under a variety of growth conditions and during different phases of the cell cycle.

2. Materials and methods

2.1. Strain isolation and growth and maintenance of the cultures

Experiments were conducted with *Gambierdiscus* sp. strain VGO917, established from seawater samples collected at Manado (Celebes Sea, SW Pacific Ocean) in 2007 and obtained by isolating a single cell in a well of a tissue-culture plate (Iwaki, Japan, 6.4-mm diameter) containing 250 μL of K/2 medium (Keller et al., 1987) without silica. The medium was prepared with Atlantic seawater adjusted to a salinity of 32 psu by the addition of sterile bi-distilled water. The plates were incubated at 25 °C, with a 12-h:12-h L:D photoperiod and an irradiance of 90 $\mu\text{mol photons m}^{-2} \text{s}^{-1}$. Culture stocks were maintained in Erlenmeyer flasks filled with 20 mL of K/2 medium and were incubated under the above-described conditions. Growth was studied in duplicate flask cultures (200 mL of medium) containing either L1 (Guillard and Hargraves, 1993), K/2 (Keller et al., 1987), or K/2 +L1 (2:1 ratio) medium, prepared and adjusted to a salinity as described above. They were placed under the same conditions used for culture maintenance. Every 2–3 days, 3-mL samples were removed from the flasks, fixed in Lugol, and used to estimate cell concentrations.

The number of cell divisions per day was calculated based on the relationship $K_e = (\ln(C_t) - \ln(C_i))/t$, where C_t and C_i are the final and the initial cell concentrations, respectively, and t = time (Guillard, 1973).

2.2. Light microscopy, cell measurements, and imaging

Experiments were performed in cultures of strain VGO917 grown in Erlenmeyer flasks (200 mL of medium) in either K/2 or K/2 +L1 (ratio 2:1) medium. Although L1 medium was used in the growth experiment, it was discarded for other measurements and imaging because after several transfers in this medium a large number of lumpy abnormal cells appeared. Two flasks were used from each medium and each one was placed in different incubators held at the same temperature but with opposite photoperiods (both 12:12 L:O), such that while one culture was in the light phase the other was in the dark phase. Two samples were collected from each incubator on each sampling day (days 2, 6, 9, and 14 from the start of the experiment), one at 09:00 and another at 14:00. Thus, samples during dark period were collected from one incubator and those from light period from the other incubator. Also, one culture was performed in K/2 +L1 medium without added nitrates, ammonium, or phosphates and placed in the incubator used for sampling in darkness. From this culture, only one sample was collected, at 14:00. Ten-mL samples were obtained from the above-described flasks on days 2, 6, 9, and 14 from the start of the experiment, immediately fixed in ethanol:acetic acid (3:1 ratio) for at least 24 h, washed twice with PBS (Sigma, USA), centrifuged, and then stained with Sybr Green (Molecular Probes, Eugene Oregon, USA) (Figueroa et al., 2006). To visualize the thecal plates, the cells were stained using the fluorescent brightener Calcofluor (Sigma) (Fritz and Triemer, 1985). An Axiocam HRC digital camera (Zeiss, Germany) was used to obtain cellular and nuclear images and measurements from cells observed by light microscopy (Leica DMR, Germany) at 630 \times magnification. Between 30 and 40 cells were analyzed in each sample. Cell size and nuclear shape were determined based on the following parameters: (1) cell area (CA), (2) cell depth (D) corresponding to the dorso-ventral diameter, (3) cell width (W) corresponding to the transverse diameter, (4) nuclear area (NA), and (5) nuclear shape index (NSI), which was calculated based from N_1 , N_2 , and N_3 as explained in Fig. 1. $NSI = N_3/N_2$. NSI was used as an indicator of nuclear shape. As shown in Fig. 1, for round or oval nuclei $NSI = 0.5$ whereas for U-shaped nuclei $NSI > 1$.

2.3. Statistical analyses

The data were analyzed using the statistical software package SPSS. Cells were classified in four groups using k-means cluster analysis based on cell depth (D) and width (W) and the nuclear shape index (NSI). The final sample comprised data from all

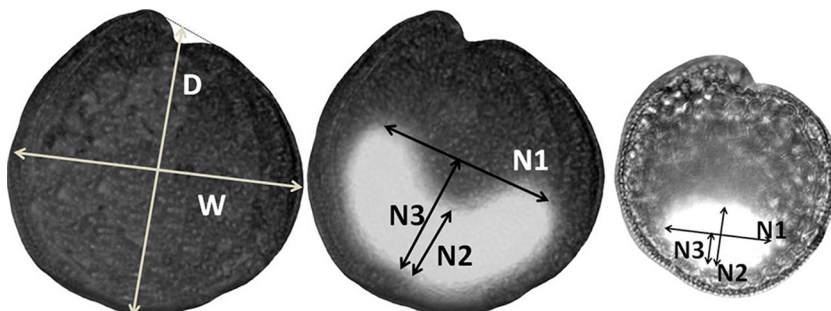


Fig. 1. Cell measurements used to estimate nuclear shape and cell size in *Gambierdiscus* sp.

samples collected from the three media ($n = 1315$). The criterion used to decide the number of clusters was based solely on the fitness of the results. Maximum interactions were set to 10. A Shapiro Wilk's test ($P > 0.05$) showed that D , W , and NSI were not normally distributed, therefore necessitating non-parametric methods (Kruskal–Wallis) to determine differences between the means. Principal component analysis (PCA) was applied to identify the underlying factors that explained the pattern of correlations within the variables CA , D , W , $N1$ and $N3$, NSI , and the type of medium (Media). NA and nuclear measurement $N2$ were excluded from the analyses because of low correlations. The final sample used for PCA consisted of the data from cells grown in the three media collected at dark at 14:00 pm ($n = 514$). Two factors with eigenvalues >1 were extracted by means of the varimax rotation method.

3. Results

3.1. Growth

Fig. 2 shows the growth curves obtained from cells grown in the three different media. The mean and standard deviation of the growth rates during the exponential phase (culture days 1–15) were: $0.31 \text{ div day}^{-1}$ ($SD = 0.06$, $n = 2$) for $K/2 + L1$, $0.19 \text{ div day}^{-1}$ ($SD = 0.13$, $n = 2$) for $K/2$, and $0.20 \text{ div day}^{-1}$ ($SD = 0.10$, $n = 2$) for $L1$.

3.2. Nuclear and cellular morphology

Table 1 lists the minimum and maximum values of the measurements (Fig. 1) and the 95% confidence interval for the mean and standard deviation. The high variability in nuclear shapes and cell sizes is evident from the wide-ranging minimum and maximum values. To study the distribution of cell size and nuclear shape, data on cell depth (D), width (W), and the nuclear shape index (NSI) were classified by cluster analyses, which defined four groups (1–4) of decreasing cell size. D and W were significantly different among groups ($P < 0.001$), with cluster 1 comprising the largest cells and cluster 4 the smallest ones (Fig. 3). The final cluster centers and the number of cases in each cluster are shown in Table 2. The NSI also decreased from group 1 to 4, with significant differences between clusters ($P < 0.01$). Small cells were associated with round or slightly U-shaped nuclei and large cells with obvious U-shaped nuclei (Fig. 3). Thus, 50% of the cells in cluster 4 had round to oval nuclei (percentile 50 of $NSI < 0.7$) and less than 10% had obvious U-shaped nuclei (percentile 90 of $NSI > 1.3$). By contrast, in cluster 1 50% of the cells had

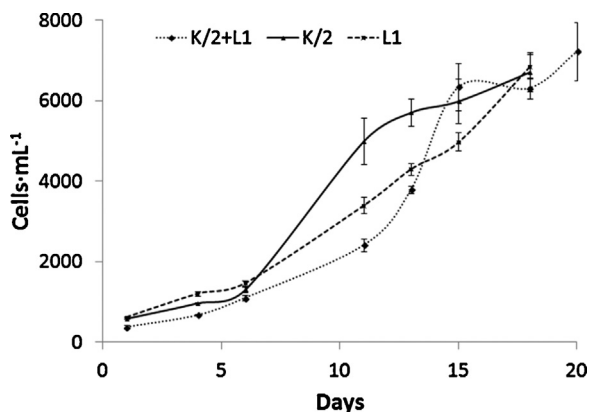


Fig. 2. Growth of *Gambierdiscus* sp. in different culture media: $K/2$ (continuous line), $L1$ (dashed line), and $K/2 + L1$ (dotted line).

Table 1

Descriptive statistics of variables of *Gambierdiscus* sp. ($n = 1315$), Cell area (CA), nuclear area (NA) cell depth (D), cell width (W), nuclear measurements ($N1$ – $N3$), nuclear shape index (NSI) (see Fig. 1 and Material and Methods).

	Minimum	Maximum	95% confidence interval of the mean	Std. deviation
CA	969	4863	2880 ± 31	566
NA	133	921	403 ± 7	137
D	32	77	57.4 ± 0.3	5
W	36	88	60.4 ± 0.4	7
$N1$	14	51	29.8 ± 0.4	7
$N2$	5	28	13.2 ± 0.1	3
$N3$	5	34	14.2 ± 0.2	5
NSI	0.3	3	1.1 ± 0.1	0.4

obvious U-shaped nuclei (percentile 50 of $NSI > 1.3$) and only 10% round to oval nuclei (percentile 10 of $NSI < 0.5$) (Fig. 3C).

Cells from clusters 1 to 4 are shown in Fig. 4. Those in cluster 1 were significantly wider than deeper, as seen from an apical or antapical view (Table 2, Figs. 3A and B, and 4A–H) whereas in cells of clusters 2, 3, and 4 cell width and depth were approximately equal (Table 2, Figs. 3A and B, and 4I–X), resulting in round cells on apical or antapical view. Most of the cells were antero–posteriorly compressed, yielding a lenticular shape, with the exception of few small globular-shaped cells (Fig. 4U–X, see Section 3.4). In all cells, independent of the cluster, the arrangement of the thecal plates was typical of lenticular *Gambierdiscus* (Fig. 4H, K, O, P, S, T, V–X).

Also shown in Fig. 4 is the large variability in nuclear shape. As represented by the NSI , U-shaped nuclei were observed in all groups, although to different degrees (Fig. 3C). Furthermore, most nuclei were dorsally located, with the exception of pre-karyokinetic and recently divided nuclei as explained in the following.

3.3. Nuclear and cellular morphology during cell division

Cells undergoing division were observed in dark-phase cultures. These cells were pre-karyokinetic, based on their centrally located, closed-U-shaped nuclei (Fig. 4C and D). Subsequently these nuclei acquired a round shape and retained their central position (Fig. 4E). Karyokinetic and cytokinetic cells (Fig. 4F and G) were also observed. Division occurred by desmoschisis in the sagittal plane, with each daughter cell inheriting half of the parental thecal plates (Fig. 4G). Very recently divided cells had a laterally positioned nucleus (Fig. 4M) which eventually moved to a dorsal position (Fig. 4N) even before thecal plates of recently divided cells were completed (Fig. 4O and P). Plate fission and separation followed the pattern described in the literature for *Gambierdiscus excentricus* (Fraga et al., 2011).

For binucleated cells, the mean \pm SD of cell depth (D) and width (W) were $65.5 \pm 6.0 \mu\text{m}$ and $71.6 \pm 5.9 \mu\text{m}$ ($n = 37$), respectively. These values were those characteristic of cells of cluster 1. For pre-karyokinetic cells (Fig. 4C–E) the values were $63.5 \pm 6.1 \mu\text{m}$ and $67.6 \pm 7.4 \mu\text{m}$ ($n = 46$) respectively, characteristic of cells in clusters 1 and 2.

Based on the presence of a round to oval nuclei in recently divided cells (Fig. 4M and N), in strain VGO917 progression of the cell cycle until division seems to involve an increase in nuclear and cellular size while at the same time the nucleus becomes U-shaped. The broad range of nuclear shapes seen in Fig. 4 reflects this process. Among samples obtained in light-phase cultures, neither karyokinetic nor binucleated cells were observed, although, like dark-phase cells, they also included cells with different forms of U-shaped nuclei.

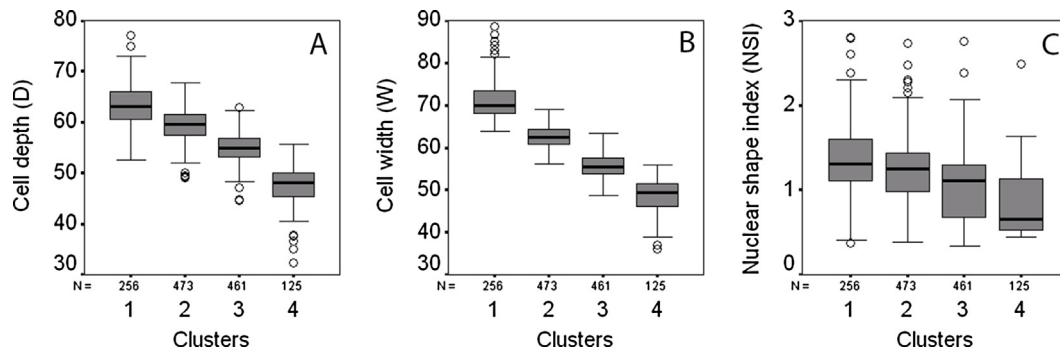


Fig. 3. Box plots of cell size (D and W) and nuclear shape index (NSI) classified by clusters.

3.4. Nuclear and cellular morphology of small cells

The smallest cells were those in cluster 4, with a confidence interval of the mean of $47.4 \pm 0.7 \mu\text{m}$ (D) and $48.3 \pm 0.7 \mu\text{m}$ (W) (Fig. 3A and B), albeit with a wide range between the minimum and maximum [32.3 (D), 31.2 (W), and 55.8 (D and W)]. Recently divided cells, characterized by their incomplete theca (Fig. 4O and P), were mostly in cluster 4, the values were $52.9 \pm 4.1 \mu\text{m}$ (D , mean \pm SD) and $49.9 \pm 3.1 \mu\text{m}$ (W , mean \pm SD) ($n = 20$).

Cluster 4 also included an abundance of cells that were smaller than the recently divided cells. A representative cell, $41 \mu\text{m}$ (D) and $39 \mu\text{m}$ (W), is shown in Fig. 4R–T. The dimensions of these cells placed them in cluster 4 but their average size was well below that of the cluster. Like the cells in the other clusters, these antero-posteriorly compressed cells were lenticular in shape, with an oval nucleus (Fig. 4R), whole theca, and a thecal plate arrangement typical of discoid *Gambierdiscus* (Fig. 4S and T), although the relatively large size of the Po plate is remarkable (Fig. 4V).

Even smaller cells ($D = 32 \mu\text{m}$ and $W = 36 \mu\text{m}$; Table 1) were observed. They were globe-shaped rather than lenticular and thus unlike all the other cells described in the present study. They were characterized by an oval nucleus (Fig. 4U) and a plate arrangement typical of discoid *Gambierdiscus* (Fig. 4V–X), but with unusual features, such as the absence of the apical Po plate as determined by optical microscopy (Fig. 4V). These cells were very scarce.

3.5. Cellular forms related to other life-cycle processes

The cellular and nuclear features of some cells could not be attributed to the division process but were likely related to sexuality. For example, a few gamete pairs were observed (Fig. 5A) and their gametes were small and thecated. In addition, there were cells in which the nucleus had a very obvious U-shape and appeared to be undergoing division at its central part (Fig. 5B), and thus unlike the nucleus of the dividing cells described in Section 3.3. The large or medium size of these cells included them in clusters 1 and 2 and their nuclear shape was suggestive of meiotic division. Since they were not abundant, with outliers SDI > 3 , they were removed from the cluster analyses.

Table 2

Final cluster centers for measurements of cell depth (D), cell width (W), and nuclear shape index (NSI) of *Gambierdiscus* sp.

Cluster	1	2	3	4
D	63.0	59.4	55.0	47.4
W	71.0	62.6	55.6	48.3
NSI	1.3	1.2	1.0	0.8
Number of specimens	260	477	462	126

Furthermore, other cells of unknown origin were observed: (1) rectangular-shaped cells with a broad ventral aspect and a laterally situated flagellar region were included in cluster 1 (Fig. 5C). The nuclei of these cells were variably shaped although generally U-shaped. (2) Large or medium size cells with an elongated nucleus (Fig. 5D) assigned based on their size to clusters 1 and 2. (3) Cells with Plates 2''' and 2''–4'' that protruded so as to form a very prominent margin (Fig. 5E). These cells were distributed among all four clusters and their nuclei were highly variable in shape, ranging from slightly to obviously U-shaped. (4) In a group of cells undergoing ecdysis, the protoplasm emerged from the theca (Fig. 5F).

3.6. Effect of nutrient-depleted medium

The effect of different media was studied by means of PCA based on the cross-correlation coefficients. The matrix for the PCA comprised the variables cellular area (CA), cell depth (D), width (W), nuclear measurements (N1 and N3), nuclear shape index (NSI) and type of medium (Media). Nuclear area and nuclear measurement N2 were excluded from the analyses because of their low correlations. Two components were extracted by the PCA that explained 74% of the variance. The Kaiser–Meyer–Olkin measure of sampling adequacy was 0.70, above the recommended value of 0.6, and Bartlett's test of sphericity (which tests for the presence of correlations among variables) was significant at $P < 0.001$. The rotated component matrix (Table 3) contained the rotated factor loadings, which explain how the variables are weighted for each factor as well as the correlation between the variables and the factor (correlations < 0.3 were not included). Only variables related to nuclear size and shape correlated positively with the type of medium (see component 2 in Table 3, which explains 25% of the variance). There was no correlation between the type of medium and cellular size (Fig. 6).

A comparison of the means of cellular and nuclear size (D , W and NSI) showed significant differences ($P < 0.001$) for variables related to nuclear shape (NSI) between the medium depleted in N and P and the other two replete media (Fig. 7A). Under nutrient limitation, the nuclei were round and seldom U-shaped (NSI > 1.1 ; see extreme values in Fig. 7A). However the sizes of cells grown in the three media did not differ (Fig. 7B and C). Large cells with round to oval dorsally located nuclei were scarce in K/2 and K/2 + L1 media, in which large cells had U-shaped nuclei, but abundant in the nutrient-depleted medium.

4. Discussion

A coherent linkage of the morphology and genetics of the *Gambierdiscus* genus has been difficult and remains problematic (Parsons et al., 2012); indeed, the morphological changes that

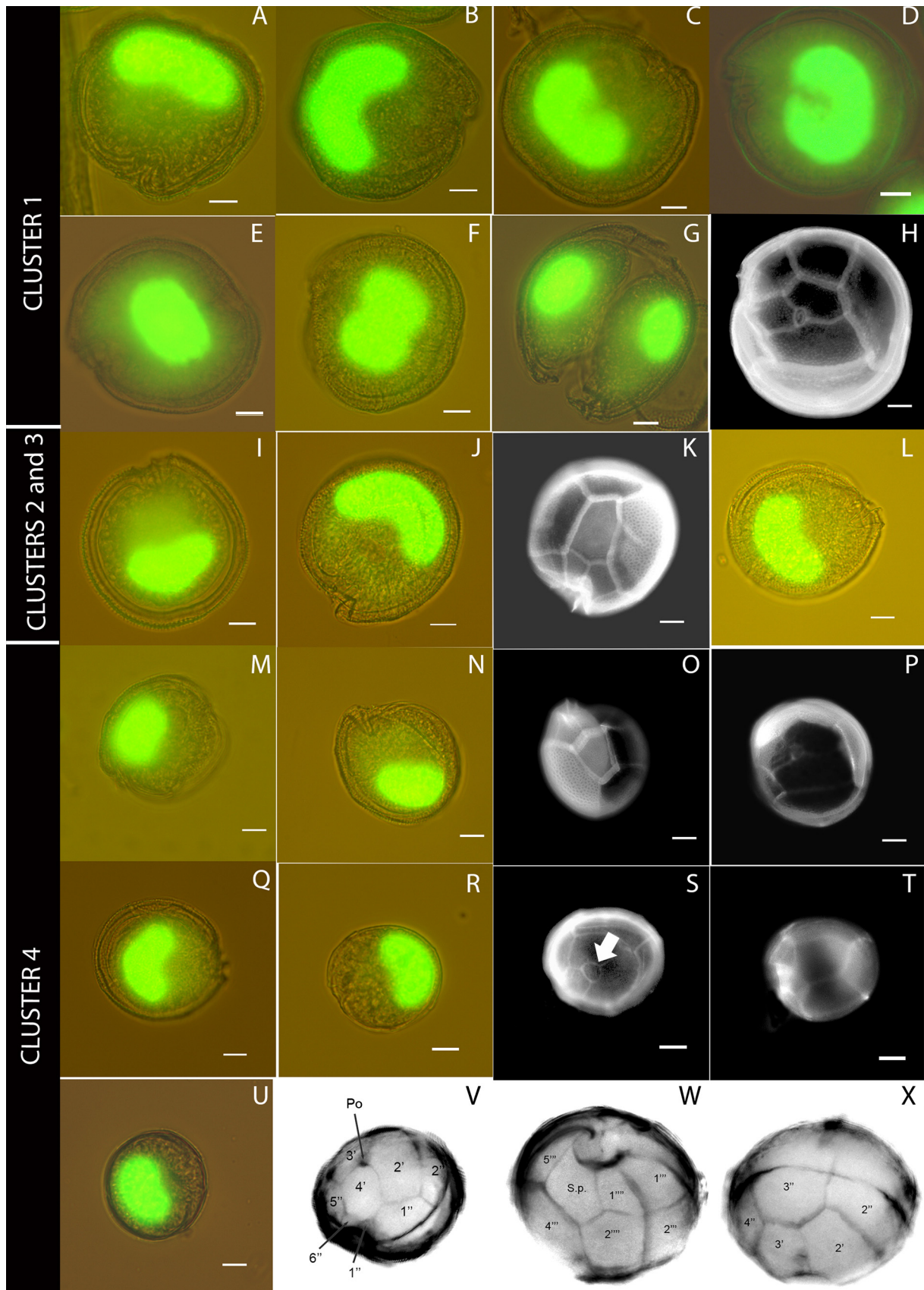


Fig. 4. Photographs of cells of *Gambierdiscus* sp. arranged according to the statistically determined four clusters. The cell nucleus before its acquisition of a U shape (A); a cell with a clearly evident U-horseshoe-shaped nucleus (B); a cell prior to karyokinesis, with a closed U-shaped nucleus (C); a cell prior to karyokinesis, with a nearly closed nucleus (D); a cell prior to karyokinesis, with a central round nucleus (E); a karyokinetic cell (F); a binucleated cell (G); calcofluor-stained epitheca with thecal plates of the same cells shown in F (H); a cluster 2 cell with an oval nucleus (I); a cluster 2 cell with a prominent U-shaped nucleus (J); calcofluor-stained hypothecha of the same cell shown in J (K); a cluster 3 cell with a slightly U-shaped nucleus (L); a very recently divided cell with half of the theca and a lateral nucleus (M); a recently divided cell

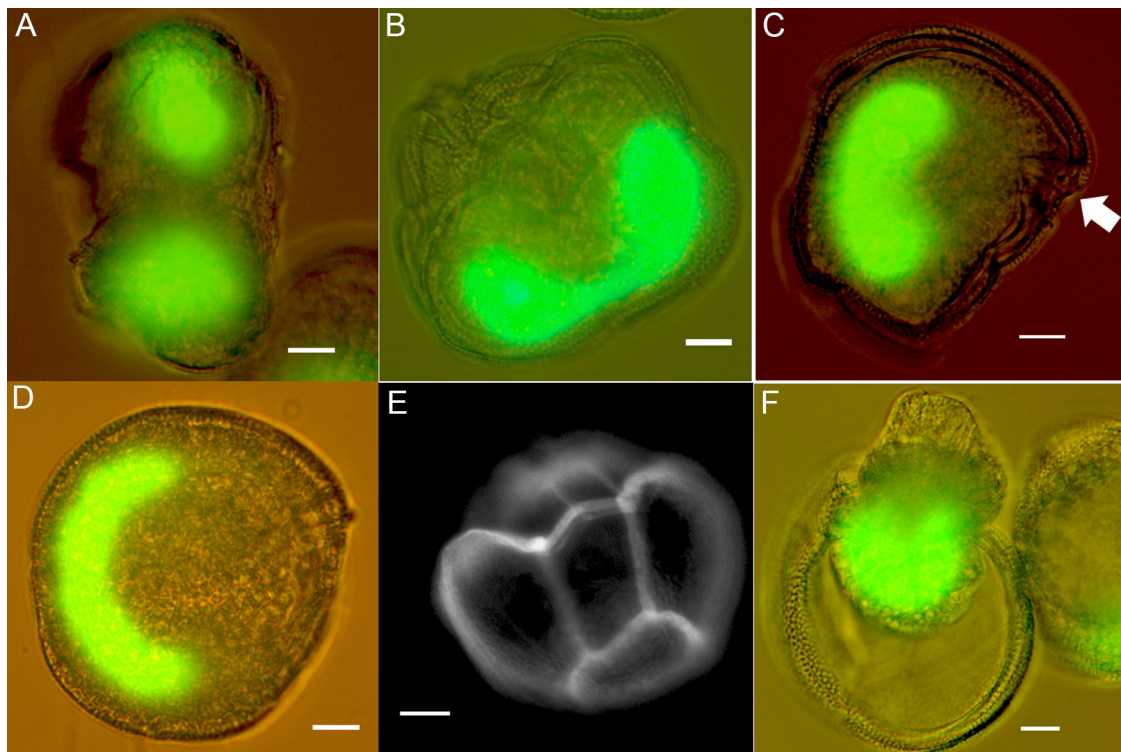


Fig. 5. *Gambierdiscus* sp. cells displayed according to life-cycle processes other than division (compare with Fig. 4). A gamete pair (A); a cell with a very obvious U-shaped nucleus that, as evident from its central part, appears to be undergoing division (B); rectangular-shaped cell with a broad ventral aspect and a laterally situated flagellar region (arrow) (C); a cell with an elongated nucleus (D); hypotheca, with the thecal plates partially protruding (E); a cell undergoing ecdysis (F).

occur during the reproduction of this dinoflagellate are almost completely unknown. In our study the intra-specific variability in size of the studied strain was greater than that reported in the *Gambierdiscus* literature. The detection of that variability was possible because of the much larger sample size (1315 specimens) than in other studies of several *Gambierdiscus* species (7–70 specimens; Chinain et al., 1999; Litaker et al., 2009; Fraga et al., 2011; Nishimura et al., 2014), which accordingly would have overlooked the very scarce smallest size cells described herein. These smallest cells (around 30 μm) displayed interesting morphological differences from the other cells, especially their globular shape rather than the lenticular shape typical of discoid *Gambierdiscus*. However, their plate arrangement was the same as that of lenticular *Gambierdiscus*. More studies of these unusual cells are needed in order to determine their origin and life-cycle function. It is extremely unlikely that they were a culture contaminant, given our efforts to ensure that the cultures used in the experiments derived from a single cell.

Small cells have been described both in cultures and field populations of many dinoflagellates (Silva and Faust, 1995). In some studies they were shown to be the gametes of certain species (Figueroa et al., 2006, 2009; Amorim et al., 2013) or were suggested to arise during the rapid asexual divisions aimed at rejuvenating the cell population (Partensky and Vaulot, 1989; Silva and Faust, 1995), but in other cases no particular function could be assigned to them (Bravo et al., 2012). In dinoflagellates, morphological differences apart from size are not common between gametes and vegetative cells; however, differences in plate tabulation and gross morphology have been reported for *Protooperidinium steidingerae*

and *Protooperidinium depressum* (Gribble et al., 2009) and for *Fragilidium subglobosum* and *F. cf. duplocampanaeforme* (Amorim et al., 2013).

Our study describes the morphological changes of *Gambierdiscus* nuclei during cell division. Similar U-shaped nuclear forms related to division were reported for *Gonyaulax tamarensis* (Dodge, 1964). In that study, the horseshoe or U-shaped form was attributed to the interphase nucleus of that species and its U-closing arms around the central body to early prophase. In the present study the intermediate forms of the U-shaped nucleus, from oval to the horseshoe-shaped interphase nucleus, presumably corresponded to S phase, i.e., to DNA replication. The many forms of these gradual transitions observed during the light phase, from the round/oval nuclei of recently divided cells (Fig. 4N) to the nearly closed nuclei of mitotic cells (Fig. 4D), suggests that most cells are in S phase during both the light phase and the dark phase. This process may be the same described in an image flow cytometry study of *Alexandrium minutum* Halim (Dapena et al., in press), in which during the light period the population was shown to be in S phase.

Here, differences in nuclear and cell size and shape and their relationship to cellular division were described in a single strain of *Gambierdiscus* sp. Morphological differences between daughter cells with respect to both size and shape were previously reported for *Gambierdiscus excentricus* (Fraga et al., 2011). These findings suggest that division-related stages in *Gambierdiscus* contribute to its known morphological intra-specific variability and thus to the difficulty in establishing morphological-genetic correspondences. However, the determination of different NSI values in all cell size

(Fig. 4 continued) with a dorsal nucleus (N); calcofluor-stained hypotheca of the same cell shown in N (O); calcofluor-stained epitheca of a recently divided cell (P); a cluster 4 cell with a U-shaped nucleus (Q); a lenticular-shaped cluster 4 cell with an oval nucleus (R); Calcofluor-stained epitheca showing the Po plate (arrow) of the same cell shown in R (S); calcofluor-stained hypotheca of the same cell shown in R (T); small globe-shaped cell with an oval nucleus (U); calcofluor-stained epitheca of the same cell shown in U (V); ventral view of the calcofluor-stained hypotheca of the same cell shown in U (W); dorsal view of the calcofluor-stained hypotheca of the same cell shown in U (X).

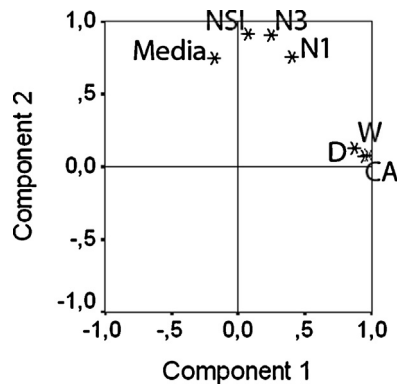


Fig. 6. Plot of the factor loading of variables used in the principal component analyses for nuclear shape, cell size, and media. CA, cell area; D, cell depth; W, cell width; N1 and N3, nucleus measurements (see Fig. 1); NSI, nuclear shape index.

groups (Fig. 3C) and the detection of cellular forms related to other life-cycle stages, as described in Section 3.5, suggest that processes other than division also account for the observed variability. The presence of gamete pairs and putative planozygotes demonstrated that sexuality occurs in cultures of *Gambierdiscus* and that the high variability in nuclear and cell shapes can be explained by the concurrence of asexual and sexual processes, as described for other dinoflagellates (von Stosch, 1973; Figueroa et al., 2006; Gribble et al., 2009; Tillmann and Hoppenrath, 2013). Thus, gametogenesis, gamete conjugation, mitosis, and meiosis together probably underlie the morphological variability depicted herein for *Gambierdiscus* sp., as these processes, by increasing or loosening DNA compaction, greatly affect nuclear size (Figueroa et al., 2014).

A proposed life cycle scheme is shown in Fig. 8, in which most of the life cycle stages described in this study are presented. Although the progression of morphological changes during division, represented in the figure as mitosis, were well distinguished herein, important gaps in our knowledge remain to be filled by further research, mainly regarding at what stage mitosis and meiosis occur. Our results provide support for the occurrence of the division process in both the sexual and the asexual cycle, and not only in the latter as traditionally understood. In our study, dividing cells were mostly in the cluster comprising the largest cells, indicating that mitosis takes place in diploid cells. Notably, life cycle processes such as meiosis and gametogenesis were previously unknown for this genus and, together with the unknown significance of the globular small cells detected in our study, highlight the need for further investigations.

Differences in the growth rates and overall health of the cells were observed between K/2, L1, and K/2 + L1 media. Although the

Table 3

Rotated component matrix of the PCA for nuclear shape and cell size variables (see Fig. 1 and Section 2) and medium type (Media).

	Component	
	1	2
CA	0.969	
D	0.832	
W	0.941	
N1	0.534	0.629
N3		0.859
NSI		0.824
Media		0.643

cultures achieved suitable growth rates in L1, the cells were abnormal in shape and therefore not used in the morphological study. L1 contains micronutrients that are not present in K/2, for example chromium, nickel, and vanadium, which may have been the cause of the cell abnormalities. Conversely, K/2 medium contains not only nitrates but also NH_4 , which, accordingly, may be necessary for the fine conditioning of *Gambierdiscus*. However, other studies on the growth of *Gambierdiscus* spp. in culture reported higher growth rates in K medium without NH_4 and Tris (Yoshimatsu et al., 2014). There is only one mention of abnormal cells in the literature, in a report on *Gambierdiscus* toxin (Holmes et al., 1990). The only modification of the K medium used in the present study was the reduction by half of all nutrients; this was done because in previous studies the lower nutrient concentration resulted in healthier cell morphology. In terms of growth, no differences were observed between K/2 and L1 media, whereas almost no growth occurred in nutrient-depleted medium. The distinct nuclear morphology in the latter medium might reflect the absence of division. Accordingly, rather than a progressive change in nuclear shape, the round to oval dorsally located nuclei suggest cellular arrest in G0 because of nutrient limitation.

Our detection of dividing cells only during dark period is consistent with the phased cell division in the diurnal cycle already reported for *Gambierdiscus toxicus* (Van Dolah et al., 1995). In that study, cell division occurred during a 3-h window beginning 6 h after the onset of the dark phase. While this pattern was described for one 24-h cycle, we were able to show that it is maintained during many days of culture, both during the early and the late phases of growth. A similar circadian regulation of cell division, with phased division during the dark period, was reported for several dinoflagellate species (Chisholm, 1981). Yet, our experience with dinoflagellate cultures has shown that in some species, for example *Alexandrium minutum* and *Ostreopsis ovata* (Figueroa et al., 2007; Bravo et al., 2012), phased division diminishes with time and division occurs also during the light phase. In culture

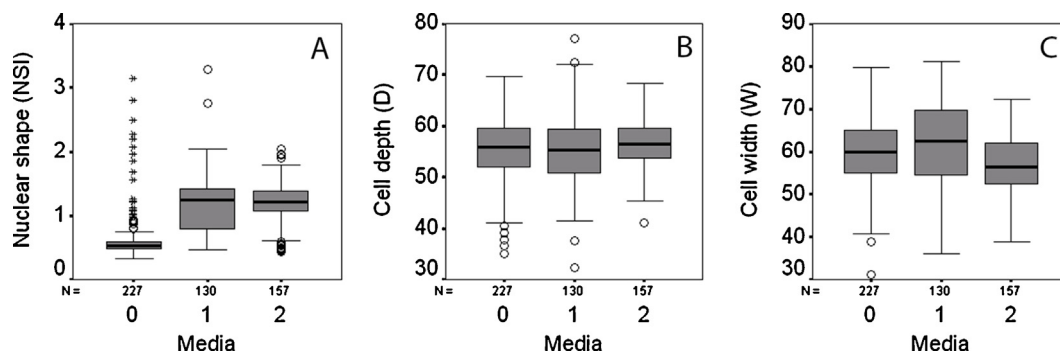


Fig. 7. Box plots of the nuclear shape index (NSI), cell depth (D), and cell width (W) in different culture media. K/2 + L1 medium without nitrates, ammonium, or phosphates (0); K/2 + L1 (1); K2 (2).

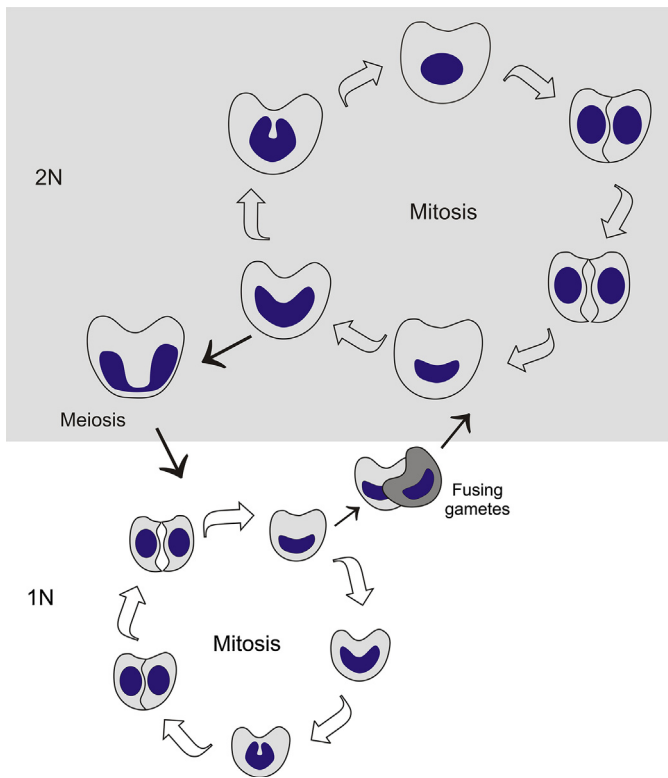


Fig. 8. Schematic drawing of proposed life cycle of *Gambierdiscus* sp.

studies of those species using synchronization methods are needed. This is in contrast to *Gambierdiscus*, in which phased division is maintained naturally over years (data not showed). Further investigations are needed to clarify whether different molecular mechanisms regulate the different cell-cycle behaviors of dinoflagellates.

Acknowledgements

We thank Alejandra Guisande Alonso for help with the cultures, technical assistance, and measurements of *Gambierdiscus*. We also thank Antonella Penna for providing the sample from which this strain was isolated, and the CCVIEO-Microalgae Culture Collection of Instituto Español de Oceanografía for providing the culture strains. This work was supported by the Spanish National project CICAN (CGL2013-40671-R). The CICAN project is sponsored by Ministry of Economy and Competitiveness (MINECO). R. Figueroa was funded by FORMAS (Sweden).[SS]

References

- Adachi, R., Fukuyo, Y., 1979. The thecal structure of the marine toxic dinoflagellate *Gambierdiscus toxicus* gen. et. sp. nov. collected in a ciguatera endemic area. *Bull. Jpn. Soc. Sci. Fish.* 45, 67–71.
- Aligizaki, K., Battochi, C., Penna, A., Rodríguez Hernández, F., Arsenakis, M., Fraga, S., 2010. Diversity of potentially toxic benthic dinoflagellates in southern Europe. In: 14th International Conference on Harmful Algae, Crete, 1–5 November, p. 25.
- Amorim, A., Veloso, V., Rodríguez, F., Fraga, S., 2013. Life-cycle, morphology and phylogeny of species of *Fragilidium* Balech from west Iberia. In: Lewis, J., Marret, F., Bradley, L. (Eds.), *Biological and Geological Perspectives of Dinoflagellates*. The Micropaleontological Society, London, pp. 215–224.
- Bravo, I., Figueroa, R.I., 2014. Towards an ecological understanding of dinoflagellate cyst functions. *Microorganisms* 1, 11–32.
- Bravo, I., Vila, M., Casablanca, S., Rodríguez, F., Rial, P., Riobo, P., Penna, A., 2012. Life cycle stages of the benthic palytoxin-producing dinoflagellate *Ostreopsis cf. ovata* (Dinophyceae). *Harmful Algae* 18, 24–34.
- Chinain, M., Faust, M.A., Pauillac, S., 1999. Morphology and molecular analyses of three toxic species of *Gambierdiscus* (Dinophyceae): *G. pacificus*, sp. nov., *G. australes*, sp. nov., and *G. polyneisiensis*, sp. nov. *J. Phycol.* 35, 1282–1296.
- Chisholm, S.W., 1981. Temporal patterns of cell-division in unicellular algae. *Can. Bull. Fish. Aquat. Sci.* 150–181.
- Dapena, C., Bravo, I., Cuadrado, A., Figueroa, R.I., in press. Nuclear and cell morphological changes during the cell cycle and growth of the toxic dinoflagellate *Alexandrium minutum*. *Protist*, in press.
- Dodge, J.D., 1964. Nuclear division in dinoflagellate *Gonyaulax tamarensis*. *J. Gen. Microbiol.* 36, 269–276.
- Elbrächter, M., 2003. Dinophyte reproduction: progress and conflicts. *J. Phycol.* 39, 629–632.
- Faust, M.A., 1995. Observation of sand-dwelling toxic dinoflagellates (Dinophyceae) from widely differing sites, including two new species. *J. Phycol.* 31, 996–1003.
- Figueroa, R.I., Bravo, I., Fraga, S., Garcés, E., Llaveria, G., 2009. The life history and cell cycle of *Kryptoperidinium foliaceum*, a dinoflagellate with two eukaryotic nuclei. *Protist* 160, 285–300.
- Figueroa, R.I., Bravo, I., Garcés, E., 2006. Multiples routes of sexuality in *Alexandrium taylori* (Dinophyceae) in culture. *J. Phycol.* 42, 1028–1039.
- Figueroa, R.I., Cuadrado, A., Stüken, A., Rodríguez, F., Fraga, S., 2014. Ribosomal DNA organization patterns within the dinoflagellate genus *Alexandrium* as revealed by FISH: life cycle and evolutionary implications. *Protist* 165 (3) 343–363.
- Figueroa, R.I., Garcés, E., Bravo, I., 2007. Comparative study of the life cycles of *Alexandrium tamutum* and *Alexandrium minutum* (Gonyaulacales, Dinophyceae) in culture. *J. Phycol.* 43, 1039–1053.
- Fraga, S., Rodríguez, F., Caillaud, A., Diogene, J., Raho, N., Zapata, M., 2011. *Gambierdiscus excentricus* sp nov (Dinophyceae), a benthic toxic dinoflagellate from the Canary Islands (NE Atlantic Ocean). *Harmful Algae* 11, 10–22.
- Fritz, L., Triemer, R.E., 1985. A rapid simple technique utilizing calcofluor white M2R for the visualization of dinoflagellate thecal plates. *J. Phycol.* 21, 662–664.
- GEOHAB, 2012. GEOHAB Core Research Project: HABs in Benthic Systems. IOC, Paris, pp. 64.
- Gribble, K.E., Anderson, D.M., Coats, D.W., 2009. Sexual and asexual processes in *Protoperidinium steidingerae* Balech (Dinophyceae), with observations on life-history stages of *Protoperidinium depressum* (Bailey) Balech (Dinophyceae). *J. Eukaryot. Microbiol.* 56, 88–103.
- Guillard, R.R.L., 1973. Division rates. In: Stein, F.R. (Ed.), *Handbook of Phycological Methods. Culture Methods and Growth Measurements*. Cambridge University Press, Cambridge, pp. 289–311.
- Guillard, R.R.L., Hargraves, P.E., 1993. *Stichochrysis immobilis* is a diatom, not a chrysophyte. *Phycologia* 32, 234–236.
- Hokama, Y., Ebesu, J.S.M., Asunson, D.A., Nagai, H., 1996. In: Yasumoto, T., Oshima, Y., Fukuyo, Y. (Eds.), *Growth and Cyclic Studies of Gambierdiscus toxicus* in the Natural Environment and in Culture. Intergovernmental Oceanographic Commission of UNESCO, Paris, pp. 313–315.
- Holmes, M.J., 1998. *Gambierdiscus yasumotai* sp.nov. (Dinophyceae), a toxic benthic dinoflagellate from southeastern Asia. *J. Phycol.* 34, 661–668.
- Holmes, M.J., Lewis, R.J., Gillespie, N.C., 1990. Toxicity of Australian and French Polynesian strains of *Gambierdiscus toxicus* (Dinophyceae) grown in culture: characterization of a new type of maitotoxin. *Toxicol.* 28, 1159–1172.
- Keller, M.D., Selvin, R.C., Claus, W., Guillard, R.R.L., 1987. Media for the culture of oceanic ultraphytoplankton. *J. Phycol.* 23, 633–638.
- Kuno, S., Kamikawa, R., Yoshimatsu, S., Sagara, T., Nishio, S., Sako, Y., 2010. Genetic diversity of *Gambierdiscus* spp. (Gonyaulacales, Dinophyceae) in Japanese coastal areas. *Phycol. Res.* 58, 44–52.
- Litaker, R.W., Vandersea, M.W., Faust, M.A., Kibler, S.R., Chinain, M., Holmes, M.J., Holland, W.C., Tester, P.A., 2009. Taxonomy of *Gambierdiscus* including four new species, *Gambierdiscus caribaeus*, *Gambierdiscus carolinianus*, *Gambierdiscus carpenteri* and *Gambierdiscus ruetzleri* (Gonyaulacales, Dinophyceae). *Phycologia* 48, 344–390.
- Litaker, R.W., Vandersea, M.W., Faust, M.A., Kibler, S.R., Nau, A.W., Holland, W.C., Chinain, M., Holmes, M.J., Tester, P.A., 2010. Global distribution of ciguatera causing dinoflagellates in the genus *Gambierdiscus*. *Toxicol.* 56, 711–730.
- Nishimura, T., Sato, S., Tawong, W., Sakanari, H., Yamaguchi, H., Adachi, M., 2014. Morphology of *Gambierdiscus scabrosus* sp nov (Gonyaulacales): a new epiphytic toxic dinoflagellate from coastal areas of Japan. *J. Phycol.* 50, 506–514.
- Parsons, M.L., Aligizaki, K., Bottein, M.-Y.D., Fraga, S., Morton, S.L., Penna, A., Rhodes, L., 2012. *Gambierdiscus* and *Ostreopsis*: reassessment of the state of knowledge of their taxonomy, geography, ecophysiology, and toxicology. *Harmful Algae* 14, 107–129.
- Partensky, F., Vaulot, D., 1989. Cell size differentiation in the bloom-forming *Gymnodinium cf. nagasakiense*. *J. Phycol.* 25, 741–750.
- Silva, E.S., Faust, M.A., 1995. Small cells in the life history of dinoflagellates (Dinophyceae): a review. *Phycologia* 34, 396–408.
- Tillmann, U., Hoppenrath, M., 2013. Life cycle of the pseudocolonial dinoflagellate *Polykrikos kofoidii* (Gymnodiniales, Dinoflagellata). *J. Phycol.* 49, 298–317.
- Van Dolah, F.M., Leighfield, T.A., Sandel, H.D.C.K.H., 1995. Cell-division in the dinoflagellate *Gambierdiscus toxicus* is phased to the diurnal cycle and accompanied by activation of the cell-cycle regulatory protein, cdc2 kinase. *J. Phycol.* 31, 395–400.
- von Stosch, H.A., 1973. Observations on vegetative reproduction and sexual life cycles of two freshwater dinoflagellates, *Gymnodinium pseudopalustre* Schiller and *Woloszynskia apiculata* sp nov. *Br. Phycol.* 105–134.
- Yoshimatsu, T., Yamaguchi, H., Iwamoto, H., Nishimura, T., Adachi, M., 2014. Effects of temperature, salinity and their interaction on growth of Japanese *Gambierdiscus* spp. (Dinophyceae). *Harmful Algae* 35, 29–37.